Calibration of Retention Volume in Size Exclusion Chromatography by Hydrodynamic Radius

Iwao Teraoka

Herman F. Mark Polymer Research Institute, Polytechnic University, 333 Jay Street, Brooklyn, New York 11201

Received March 15, 2004; Revised Manuscript Received June 18, 2004

ABSTRACT: Universal calibration of retention volume in size exclusion chromatography (SEC) is examined using Gaussian chain models for linear and branched chain polymers. The question is which molecular dimension, the radius of gyration R_g or the hydrodynamic radius R_H, determines the partitioning of polymers of different architectures. The partition coefficient K is calculated for asymmetric star polymers, two-branch-point polymers, and comb polymers with a pore of slit geometry of opening d. The plots of K as a function of R_H/d for these polymers nearly overlap with each other, whereas the agreement is poorer for the plots of K as a function of R_g/d. The experimental data of the SEC retention volume recently obtained by Sun et al. for linear and branched polyethylene [*Macromolecules* **2004**, *37*, 4304] are used to demonstrate that the quality of the calibration curve using R_H is superior to the one using R_g and comparable to the one using hydrodynamic volume widely practiced in the community. The universal calibration by R_H will facilitate inferring the branching structure of a given chain polymer from its SEC retention volume, since calculation of R_H is much easier for any chain architecture compared with the hydrodynamic volume.

1. Introduction

Size exclusion chromatography (SEC) is one of the most frequently used characterization methods for synthetic and natural polymers.[1] The recent progress in inline detectors such as multiangle light scattering detectors and viscosity detectors has transformed SEC into an all-round solution characterization method producing the relationship between the molecular weight (MW) M, intrinsic viscosity $[\eta]$, and the radius of gyration R_g in a mere 30 min.

Since the seminal work by Grubisic et al.,[2] it has been recognized that various linear polymers and polymers of different architectures follow a so-called universal calibration curve,[3,4] once the SEC system with columns is specified. The universal calibration relates the retention volume V_R of a given fraction of a polymer to the hydrodynamic volume of that fraction which is given as $[\eta]M$. The presence of the universal calibration curve indicates that polymer molecules are partitioned between the pore and the interstitial volume within an SEC column according to the hydrodynamic volume. Since the latter is a dynamic quantity and the partitioning is an equilibrium property, the universality of the curve has been puzzling to researchers for decades.[5] They would rather associate the partition coefficient to the chain dimension defined for a static conformation, such as R_g, if possible.

Recently, Sun et al.[5] compared the universality of the relationship between V_R and R_g and the one between V_R and $[\eta]M$ for linear polystyrene, linear polyethylene, and branched polyethylene of different architectures such as a star, a two-branch point star, and a comb. They found that the two linear polymers follow a common curve when V_R is plotted as a function of R_g in the whole range of MW that spans 3 orders of magnitude. When V_R was plotted as a function of $[\eta]M$, however, the agreement between the two series of V_R data was not as good, especially toward the low end of the MW range studied. The situation was rather reversed when V_R of the linear and branched polyethylene were compared. The agreement was better in the plot of V_R as a function of $[\eta]M$, although there were some deviations.

Theoretical studies on the partitioning of polymer chains were initiated by Casassa's group many decades ago.[6,7] They calculated the partition coefficient K of a linear polymer and a star polymer of a Gaussian conformation in equilibrium with pores of various geometries. The purpose of the calculation was to associate K with R_g/d, where d is the pore size. They found that the plots of K as a function of R_g/d for star polymers of different numbers of arms do not follow a common curve. In an effort to bring these plots into a universal relationship, they proposed using $(R_g/d)g^{-1/3}$ in place of R_g/d, where g is the ratio of R_g^2 of the branched polymer to R_g^2 of a linear counterpart of the same mass, but the success was limited. They also showed,[7] based on the ratio of the intrinsic viscosity of the star polymer to that of the linear polymer of the same mass,[8,9] that $(R_g g^{-1/3})^3$ is close to the hydrodynamic volume (per molecule), indicating equivalence between the plot of K vs $(R_g/d)g^{-1/3}$ and the SEC universal calibration by $[\eta]M$.

There are several measures for the linear dimension of a polymer. Among others, R_g and the hydrodynamic radius R_H are commonly used since they are defined for polymers of different architectures and can be determined in light scattering experiments. In the present paper, we follow Casassa's method[7] to extend the calculation of K to asymmetric star polymers, two-branch-point polymers, and comb polymers of Gaussian conformation. We demonstrate that using R_H to represent the linear dimension of the polymer molecule rather than R_g gives a better universality in the plot of K as a function of the chain dimension relative to the pore size. A better universality is also shown for the SEC data obtained by Sun et al.[5]

10.1021/ma0494939 CCC: $27.50
Published on Web 07/29/2004

Recently, Radke[10,11] performed computer simulation studies to calculate the sizes of star polymers and comb polymers and, using these results, estimate their partition coefficients in a spherical pore. He pointed out that the partition coefficient in the pore of a given radius is a universal function of R_H for these polymers.

2. Chain Dimensions

We adopt a simple model of a polymer molecule: beads of the same size are connected by massless bonds to form a desired chain architecture. Let $\mathbf{r}_n$ ($n = 1, 2, ..., N$) be the position of the nth bead in the molecule that consists of N beads. For this model, R_g is given as[12]

$$2R_g^2 = N^{-2} \sum_{m,n=1}^{N} \langle (\mathbf{r}_m - \mathbf{r}_n)^2 \rangle_{mn} \qquad (1)$$

where $\langle f(\mathbf{r}_m,\mathbf{r}_n)\rangle_{mn}$ denotes the statistical average of $f(\mathbf{r}_m,\mathbf{r}_n)$, a function of $\mathbf{r}_m$ and $\mathbf{r}_n$, for a given pair of beads, m and n.

Assuming the Oseen tensor for the hydrodynamic interaction between the beads in the molecule (Kirkwood approximation[13]), R_H is expressed as[12]

$$R_H^{-1} = N^{-2} \sum_{m,n=1}^{N} \langle |\mathbf{r}_m - \mathbf{r}_n|^{-1} \rangle_{mn} \qquad (2)$$

Pairs of $m = n$ are excluded from the sum. Experimentally, R_H is determined from the Stokes−Einstein diffusion coefficient which is obtained in dynamic light scattering experiments.

Comparison of eqs 1 and 2 reveals that R_g is heavily weighted by a distant pair of beads in an instantaneous conformation of the polymer molecule whereas a pair in the close vicinity dominates the averaging for R_H. Thus, R_H is more sensitive, than R_g is, to the bulkiness of the central portion of the branched polymer molecule where the branching crams the beads.

It has been pointed out that a polymer molecule with its linear dimension greater than the pore opening can enter the pore without difficulty by placing the largest dimension parallel to the pore walls.[14,15] The extreme case is a rodlike molecule.[16] Its partition coefficient decreases only algebraically with increasing its length as opposed to the exponential decrease seen for a random-coil molecule.[17] These facts lead to a conclusion that the partitioning is more strongly influenced by the size of the core portion of the polymer molecule and not as much by its "outliers". Then, R_H may be a better measure of the chain dimension for the partitioning than R_g is.

In the present report, we replace the sums in eqs 1 and 2, for simplicity, with integrals. When a linear portion of the branched polymer, that is, an arm or a portion between adjacent branching points, contains sufficient numbers of beads, the integrals give good approximations.

Although dynamic in origin, eq 2 allows R_H to be computed for a static conformation of the molecule. In contrast, computation of $[\eta]$ in the model requires an additional assumption on the movement of each bead in a viscous solvent. Furthermore, calculation of $[\eta]$ for different chain architectures is more difficult compared with R_H. In fact, $[\eta]$ has been calculated only for linear and symmetric star polymers.[9] In contrast, R_H was calculated for chains of more complicated architectures including comb polymers.[18]

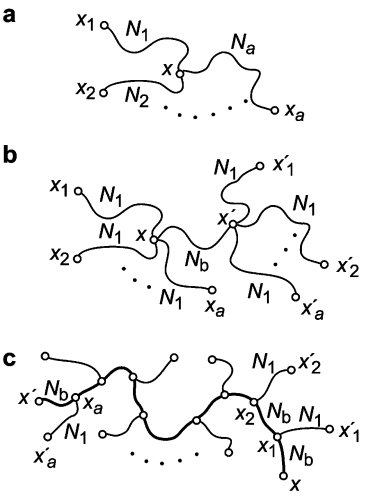

Figure 1. Three architectures of branching: (a) a-arm star polymer, (b) two-branch-point polymer, and (c) a-arm comb polymer.

It is known experimentally that $[\eta]M/R_H^3$ is nearly identical to polymers of different architectures.[19] Theoretical proof was given by Zimm and co-workers, who applied the normal-mode analysis with hydrodynamic interactions present between beads to linear polymers and star polymers.[8,9] It is common to these two architectures that $[\eta]M \propto \Sigma_i \tau_i$, where τ_i is the relaxation time of the ith normal mode ($i = 1, 2, ...$). The sum of τ_i is dominated by τ_1, which depends on the total number of beads of the molecule in the same way as R_H^3 does. Both τ_1 and R_H are governed by the global architecture of the molecule rather than local details. Therefore, we can expect that R_H will be an alternative to the cubic root of the hydrodynamic volume. The latter may include the SEC universal calibration curve.

3. Branching Parameters

Branching parameters are widely being used to describe the degree of branching. The branching parameter compares the squared dimensions of a branched polymer and a linear polymer that consist of the same repeating units and have the same total number of repeating units. For radius of gyration, the branching parameter g is defined as[12]

$$g = R_g^2/R_{gl}^2 \qquad (3)$$

where R_g^2 and R_{gl}^2 are the mean-square radii of gyration of the branched polymer and the linear polymer, respectively. Likewise, we define the branching parameter g_H for the hydrodynamic radius as[12]

$$g_H = R_H^2/R_{Hl}^2 \qquad (4)$$

where R_H and R_{Hl} are the hydrodynamic radii of the branched polymer and the linear polymer, respectively.

In the present report, we consider three architectures of branching as illustrated in Figure 1. In (a) for an a-arm star polymer, we allow asymmetricity by assigning a different number of beads (or bonds), N_i, to each of the a arms ($i = 1, 2, ..., a$). In (b) for a two-branch-point polymer, we assume for simplicity that the two branch points have the same number (a) of branches, and these $2a$ branches have the same number of beads

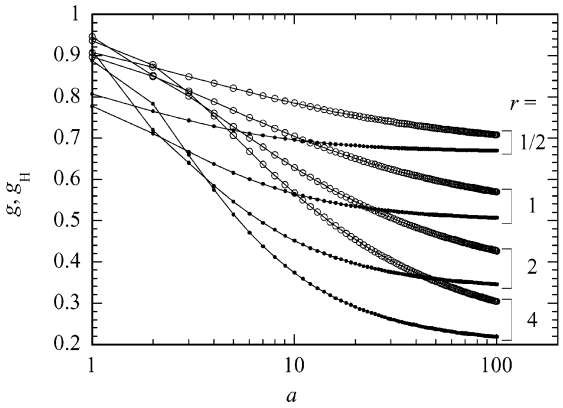

Figure 2. Comparison of g (dots) and g_H (open circles) for comb polymers with $r = N_1/N_b = 1/2$, 1, 2, and 4. The two branching parameters are plotted as a function of a, the number of combs. Although lines are drawn, the data are meaningful only at integral values of a.

(bonds), N_1. The bridge between the two branch points has N_b bonds. In (c) for a comb polymer, we assume that each arm has N_1 beads (bonds), and the grafting points are equally spaced by N_b bonds on the backbone. The mean distance between adjacent beads is assumed to be b in all of the architectures.

We assume Gaussian chain statistics for any linear part of the polymer molecule either along an arm or along the backbone. Namely, $\mathbf{r}_m$ and $\mathbf{r}_n$, the positions of the mth and nth beads in the polymer molecule separated by l bonds along the linear part, are distributed with

$$G_0(\mathbf{r}_m, \mathbf{r}_n; l) = (2\pi lb^2/3)^{-3/2} \exp[-3(\mathbf{r}_m - \mathbf{r}_n)^2/(2lb^2)] \quad (5)$$

For the three chain architectures, g was calculated as[5,20,21]

$$g_{\text{star}} = \frac{3}{N^2}\sum_{i=1}^{a} N_i^2 - \frac{2}{N^3}\sum_{i=1}^{a} N_i^3 \quad (6)$$

$$g_{\text{2br}} = \frac{(12a^2 - 4a)r^3 + 6ar(ar + 1 + r) + 1}{(1 + 2ar)^3} \quad (7)$$

$$g_{\text{comb}} = \frac{a(3a - 2)r^3 + a(a + 1)[(a + 2)r^2 + (2a + 1)r] + (a + 1)^3}{(ar + a + 1)^3} \quad (8)$$

where N is the total number of beads in the polymer and $r = N_1/N_b$. For a symmetric star ($N_i = N_1$), eq 6 reduces to $g_{\text{star}} = 3/a - 2/a^2$.

Since there are no references available for g_H, we calculated it for the three architectures. The results, together with details of calculation, are shown in Appendices A−C.

To see how g and g_H are different, we show in Figure 2 the two parameters for the comb polymer as a function of a for $r = N_1/N_b = 1/2$, 1, 2, and 4. In the asymptote of $a \to \infty$, both parameters approach $1/(1 + r)$; the polymer is just a linear polymer chain that has more mass per length of the backbone than does the linear reference polymer. At each of the four values of r, g_H approaches its asymptote much more slowly than g does, a result ascribed to the bulkiness of the comb polymer around its backbone.

4. Partition Coefficients

We obtain expressions of the partition coefficient for the three architectures of branching using the molecular parameters given in Figure 1. For each chain architecture, a polymer molecule of a Gaussian conformation is constructed part by part by growing an arm or a section between adjacent grafting points on the backbone. Each part is described by the Gaussian function, eq 5. The partition coefficient of such a molecule with a pore space is equal to the probability to contain all parts of the polymer without touching the pore walls, starting at an arbitrary point within the space. In the slit geometry of pore specified by $0 < x < d$ and extending in the y and z directions, only the x component of the conformation matters. We intend to derive expressions of the partition coefficient friendly to numerical computation.

We limit the pore geometry to a slit. The slit geometry is sufficient for the purpose of comparing how the partition coefficient depends on the chain dimension relative to the pore size for different branching architectures. The difference of the dependence is parallel in different pore geometries.[7] The partition coefficient in a channel of a square cross section of $d \times d$, for instance, is equal to the square of the partition coefficient in the slit of width d.[22]

(1) *K* of an Asymmetric Star Polymer. As shown in Figure 1a, the branching point of the a-arm star polymer is at x, and the end point of the ith arm is at x_i ($i = 1, 2, ..., a$). Then, its partition coefficient K_s is calculated as[7,23]

$$K_s = \frac{1}{d}\int_0^d \mathrm{d}x \int_0^d \mathrm{d}x_1 \cdots \int_0^d \mathrm{d}x_a\, G(x,x_1;N_1)...G(x,x_a;N_a) \quad (9)$$

where $G(x,x_i;N_i)$ is the Green function for the ith arm. In the slit, any linear part of a Gaussian chain consisting of n bonds of length b and having its ends at x and x' has the Green function $G(x,x';n)$ given as

$$G(x,x';n) = \sum_{k=1}^{\infty} u_k(x)\, u_k(x') \exp(-n\epsilon_k) \quad (10)$$

with the normalized eigenfunctions

$$u_k(x) = (2/d)^{1/2} \sin(k\pi x/d) \quad (k = 1, 2, ...) \quad (11)$$

and the eigenvalues

$$\epsilon_k = (b^2/6)(k\pi/d)^2 = \epsilon_1 k^2 \quad (12)$$

We use the running index k_i for the ith arm. Using eqs 10 and 11, eq 9 is rewritten to

$$K_s = \frac{1}{d}\sum_{k_1=1}^{\infty} \exp(-N_1\epsilon_{k_1})... \sum_{k_a=1}^{\infty} \exp(-N_a\epsilon_{k_a}) \int_0^d u_{k_1}(x)...u_{k_a}(x)\, \mathrm{d}x \int_0^d u_{k_1}(x_1)\, \mathrm{d}x_1 ... \int_0^d u_{k_a}(x_a)\, \mathrm{d}x_a \quad (13)$$

The integral with respect to x_1 is calculated as

$$\sum_{k_1=1}^{\infty} \exp(-N_1\epsilon_{k_1})\int_0^d \mathrm{d}x_1\, u_{k_1}(x_1) = \frac{2(2d)^{1/2}}{\pi} \sum_{k_1:\mathrm{odd}} \frac{1}{k_1} \exp(-N_1\epsilon_{k_1}) \quad (14)$$

The integrals with respect to x_2, ..., x_a are calculated in the same way. Therefore

$$K_s = 2\left(\frac{2}{\pi}\right)^a \sum_{k_1:\mathrm{odd}} \frac{1}{k_1} \exp(-N_1\epsilon_{k_1}) \cdots \sum_{k_a:\mathrm{odd}} \frac{1}{k_a} \exp(-N_a\epsilon_{k_a}) I_{k_1\cdots k_a} \quad (15)$$

where

$$I_{k_1\cdots k_a} \equiv (2d)^{a/2-1}\int_0^d u_{k_1}(x)\cdots u_{k_a}(x)\,\mathrm{d}x \quad (16)$$

Apparently, $I_{k_1\cdots k_a}$ is invariant to permutation of k_1, ..., k_a. Calculations of $I_{k_1\cdots k_a}$ are shown in Appendix D. When all N_i are identical, eq 15 is the same as the result obtained by Casassa and Tagami.[7] Equation 15 with $a = 2$ gives K_s that is identical to the partition coefficient of a linear chain of $N_1 + N_2$ beads.

(2) *K* of a Symmetric Two-Branch-Point Polymer. As shown in Figure 1b, the bridge of N_b bonds has its two ends at x and x'. From the end at x, a arms, each with N_1 beads, grow to end at x_1, ..., x_a. Likewise, from the end at x', a arms of N_1 beads grow to end at x'_1, ..., x'_a. The partition coefficient K_{2br} of this polymer is given as

$$K_{2br} = \frac{1}{d}\int_0^d\mathrm{d}x\int_0^d\mathrm{d}x'\, G(x,x';N_b)\Big[\int_0^d\mathrm{d}x_1\cdots \int_0^d\mathrm{d}x_a\, G(x_1,x;N_1)\cdots G(x_a,x;N_1)\Big]\Big[\int_0^d\mathrm{d}x'_1\cdots \int_0^d\mathrm{d}x'_a\, G(x',x'_1;N_1)\cdots G(x',x'_a;N_1)\Big] \quad (17)$$

We use running index k_b for the bridge and rewrite eq 17 to

$$K_{2br} = \frac{1}{d}\sum_{k_b=1}^{\infty} \exp(-N_b\epsilon_{k_b})\Big[\int_0^d u_{k_b}(x)\,\mathrm{d}x\int_0^d\mathrm{d}x_1\cdots \int_0^d\mathrm{d}x_a\, G(x_1,x;N_1)\cdots G(x_a,x;N_1)\Big]^2 \quad (18)$$

We use running index k_i for the ith arm for the Green functions in eq 18. Calculation proceeds in the same way as for K_s. We obtain

$$K_{2br} = 2\left(\frac{2}{\pi}\right)^{2a} \sum_{k_b:\mathrm{odd}}^{\infty} \exp(-N_b\epsilon_{k_b})\left[\sum_{k_1:\mathrm{odd}}^{\infty} \frac{1}{k_1} \exp(-N_1\epsilon_{k_1})\cdots \sum_{k_a:\mathrm{odd}}^{\infty} \frac{1}{k_a} \exp(-N_1\epsilon_{k_a}) I_{k_b k_1\cdots k_a}\right]^2 \quad (19)$$

(3) *K* of a Comb Polymer. As shown in Figure 1c, the backbone of $(a + 1)N_b$ bonds has grafting points, each separated by N_b bonds, at x_1, x_2, ..., x_a. The terminals of the backbone are at x and x'. From the ith graft point at x_i, an arm of N_1 beads grows to reach x'_i. The partition coefficient K_c of such a molecule is given as

$$K_c = \frac{1}{d}\int_0^d\mathrm{d}x\int_0^d\mathrm{d}x'\int_0^d\mathrm{d}x_1\int_0^d \mathrm{d}x'_1\int_0^d\mathrm{d}x_2\int_0^d\mathrm{d}x'_2\cdots \int_0^d\mathrm{d}x_a\int_0^d\mathrm{d}x'_a\, G(x,x_1;N_b)G(x_1,x'_1;N_1)\, G(x_1,x_2;N_b)\, G(x_2,x'_2;N_1)\cdots G(x_{a-1},x_a;N_b)\, G(x_a,x'_a;N_1)\, G(x_a,x';N_b) \quad (20)$$

We use running index k_1 for $G(x,x_1;N_b)$, k_i ($i = 2$, ..., a) for $G(x_{i-1},x_i;N_b)$, k'_i ($i = 1, 2$, ..., a) for $G(x_i,x'_i;N_1)$, and k for $G(x_a,x';N_b)$. As for K_s and K_{2br}, we can rewrite eq 20 to

$$K_c = 2\left(\frac{2}{\pi}\right)^{2a+2} \sum_{k_1:\mathrm{odd}}^{\infty} \frac{1}{k_1} \exp(-N_b\epsilon_{k_1}) \sum_{k'_1:\mathrm{odd}}^{\infty} \frac{1}{k'_1} \exp(-N_1\epsilon_{k'_1}) \sum_{k_2:\mathrm{odd}}^{\infty} \exp(-N_b\epsilon_{k_2}) \sum_{k'_2:\mathrm{odd}}^{\infty} \frac{1}{k'_2} \exp(-N_1\epsilon_{k'_2})\cdots \sum_{k_a:\mathrm{odd}}^{\infty} \exp(-N_b\epsilon_{k_a}) \sum_{k'_a:\mathrm{odd}}^{\infty} \frac{1}{k'_a} \exp(-N_1\epsilon_{k'_a}) \sum_{k:\mathrm{odd}}^{\infty} \frac{1}{k} \exp(-N_b\epsilon_k)\left(\frac{\pi}{2}I_{k_1k'_1k_2}\right)\left(\frac{\pi}{2}I_{k_2k'_2k_3}\right)\cdots \left(\frac{\pi}{2}I_{k_{a-1}k'_{a-1}k_a}\right)\left(\frac{\pi}{2}I_{k_ak'_ak}\right) \quad (21)$$

which is simplified to a $(a + 1)$-fold sum of a-fold products of two-dimensional arrays:

$$K_c = 2\left(\frac{2}{\pi}\right)^{2a+2} \sum_{k_1:\mathrm{odd}}^{\infty} \frac{1}{k_1} \exp(-N_b\epsilon_{k_1}) \sum_{k_2:\mathrm{odd}}^{\infty} \exp(-N_b\epsilon_{k_2})\cdots \sum_{k_a:\mathrm{odd}}^{\infty} \exp(-N_b\epsilon_{k_a})\times \sum_{k:\mathrm{odd}}^{\infty} \frac{1}{k} \exp(-N_b\epsilon_k) J_{k_1k_2}J_{k_2k_3}\cdots J_{k_{a-1}k_a}J_{k_ak} \quad (22)$$

where

$$J_{k_ik_{i+1}} = \sum_{k'_i:\mathrm{odd}}^{\infty} \frac{1}{k'_i} \exp(-N_1\epsilon_{k'_i})\frac{\pi}{2}I_{k_ik'_ik_{i+1}} \quad (i = 1, \ldots, a \text{ with } k_{a+1} = k) \quad (23)$$

is symmetric for the exchange of k_i and k_{i+1}. Equation 22 can be further simplified by taking every other sum, for instance, the sum with respect to k_2 gives another two-dimensional array:

$$\sum_{k_2:\mathrm{odd}}^{\infty} \exp(-N_b\epsilon_{k_2})J_{k_1k_2}J_{k_2k_3} = L_{k_1k_3} \quad (24)$$

Then, the number of the two-dimensional arrays in the sum decreases to about $^1/_2$ of the one in eq 22. Repeating this procedure, eq 22 eventually reduces to a 2-fold sum of the elements in a two-dimensional array. Therefore, the cost of computation increases only in proportion to the logarithm of a.

To verify consistency of eqs 19 and 22, we calculated K_{2br} and K_c, for both $N_b = N_1$ and $a = 2$. The results were identical. We also verified numerically that eq 22, in the asymptote of $N_1 \to 0$, gives the same partition coefficient as that of a linear chain of $(a + 1)N_b$ bonds.

(4) Universality of Partition Coefficients. Having obtained the expressions convenient for numerical

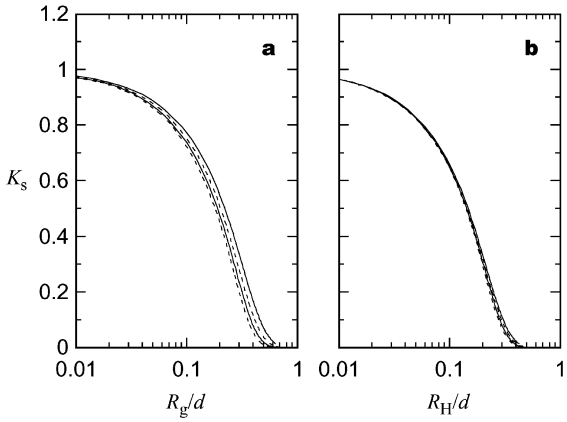

Figure 3. Partition coefficients K_s for symmetric star polymers of 2, 3, 4, and 5 arms (from top to bottom) with a slit of width d, plotted as a function of (a) R_g/d and (b) R_H/d. Alternate solid and dashed lines are used to distinguish the lines.

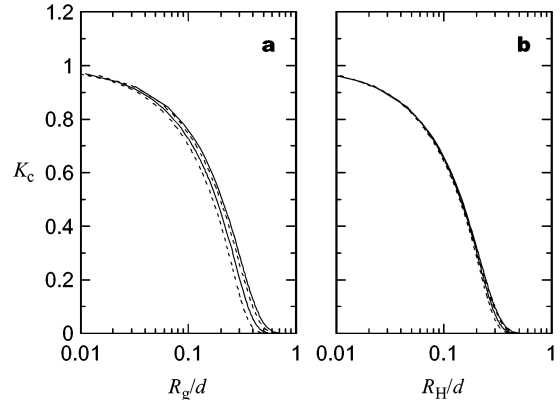

Figure 4. Partition coefficients K_c of comb polymers with a slit of width d, plotted as a function of (a) R_g/d and (b) R_H/d. From top to bottom, $r = N_1/N_b = 1$, $a = 100$; $r = 1$, $a = 20$; $r = 2$, $a = 20$; and $r = 4$, $a = 20$.

computation, we examine the universality of the partition coefficients. First, we compare K_s of symmetric 2-, 3-, 4-, and 5-arm star polymers. The two-arm star is essentially a linear polymer. Parts a and b of Figure 3 compare K_s as a function of R_g/d and R_H/d, respectively. In part a, increasing the number of arms makes the penetration into the pore more difficult, compared at the same R_g/d, a result ascribed to the bulkiness in the core portion of the polymer. Adding arms does not increase R_g so much, although it decreases the probability of containing all parts of the polymer within the slit space. The large difference between different numbers of arms is drastically reduced in part b. Adding another arm increases R_H more than it does R_g since the segment density in the core portion increases, a situation that parallels to the decrease in K_s. The two parts of Figure 3 indicate that R_H/d is superior to R_g/d to estimate the confinement strength.

Second, we examine the universality between different comb polymers. For demonstration, K_c was calculated for comb polymers with $r = N_1/N_b = 1$, $a = 100$; $r = 1$, $a = 20$; $r = 2$, $a = 20$; and $r = 4$ and $a = 20$. Comb polymers with a greater r have more mass per length of the chain backbone. Calculation results are compared in the two parts of Figure 4. The difference we have seen in the two parts of Figure 3 is repeated here. Namely, comb polymers with more mass around the chain backbone find it more difficult to enter the pore, compared at the same R_g/d. In the plot as a function of R_H/d, the large difference is greatly reduced. The universality is better in part b.

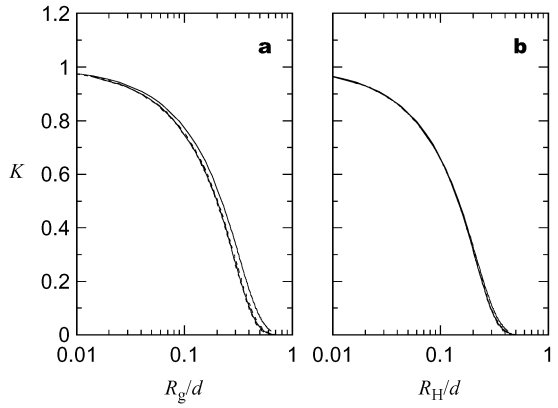

Figure 5. Comparison of the partition coefficients of different architectures, plotted as a function of (a) R_g/d and (b) R_H/d. From top to bottom, the architecture is a linear polymer, a symmetric 3-arm star polymer, a symmetric two-branch-point, 2-arm polymer ($N_1/N_b = 1$), and a comb polymer ($N_1/N_b = 1$, $a = 20$).

Last, the universality is examined for polymers of different architectures. Parts a and b of Figure 5 compare the plots of the partition coefficient for a linear polymer, a symmetric star polymer, a symmetric two-branch-point polymer, and a comb polymer. Trifunctional branching was enforced in every branching point of the three branching architectures. We chose $N_1/N_b = 1$ and $a = 2$ for the two-branch-point polymer and $N_1/N_b = 1$ and $a = 20$ for the comb polymer.

The universality in part b of the three figures could be improved by plotting K as a function of $(R_H/d)g_H^{\alpha}$ with an exponent α common to different branching geometries, as Casassa and Tagami[7] did in their universality plot as a function of $(R_g/d)g^{-1/3}$. However, expressing the confinement strength as a function of a simple ratio of the linear dimension to the pore size without a correction factor is appealing; there is no need to know R_H of the linear polymer that consists of the same repeating units and has the same molecular weight as those of the branched polymer.

A different measure of the chain dimension, such as $\langle|\mathbf{r}_m - \mathbf{r}_n|^{\beta}\rangle^{1/\beta}$ with β other than 2 or -1, could be also explored to find the optimal β that optimizes the overlapping of all the plots of the partition coefficients as a function of $\langle|\mathbf{r}_m - \mathbf{r}_n|^{\beta}\rangle^{1/\beta}/d$. However, experimental methods to evaluate the dimension are available only for $\beta = 2$ and -1 at this moment. Thus, we conclude that, for all practical reasons, R_H/d gives a good measure of the confinement strength for Gaussian chain molecules of different branching architectures. Our conclusion is consistent with the one drawn by Radke.[10,11]

The universality does not include spheres and rigid rods. For a sphere of radius R_H, $K = 1 - 2R_H/d$. It is apparent that the plot of K does not fall near the lines for chains molecules in Figure 5. Likewise, it can be shown that there is a distance between the plot of K vs R_H for a rigid rod and the plots for the chain molecules. Deviation was also noted by Casassa in the universal calibration by $[\eta]M$.[24]

5. Calibration Using Experimental Data

It is interesting to see how well the universal calibration by R_H fares in experimental results compared with the one by R_g. Here we use the data of R_g and the SEC

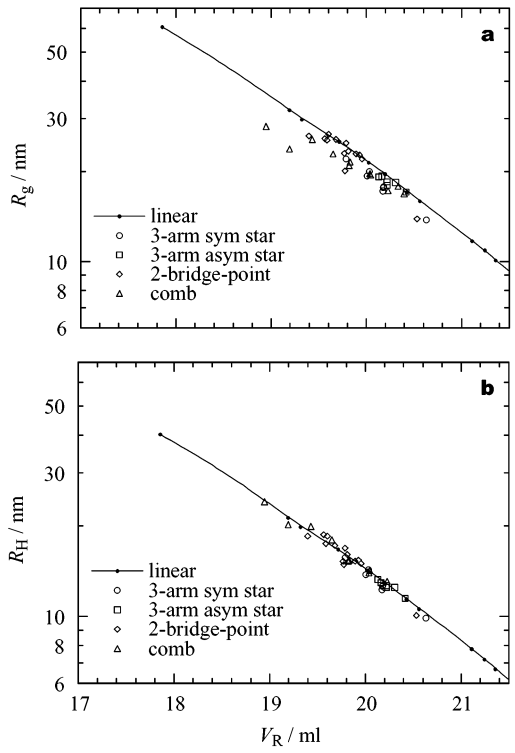

Figure 6. Calibration curve for the SEC retention volume V_R of linear and branched polyethylene using (a) R_g and (b) R_H. Branching architectures are symmetric three-arm star, asymmetric three-arm star, symmetric two-bridge-point polymer, and comb polymer. Data of V_R and R_g by Sun et al. (ref 5). Lines fit the data for linear polyethylene.

retention volume V_R obtained by Sun et al. in their study of the universal calibration for linear polyethylene and branched polyethylene of different branching architectures.[5] Comb polymers with less than three arms are excluded here. Since R_H was not measured, we use

$$R_H/R_g = (g_H/g)^{1/2}(R_{Hl}/R_{gl}) = (3\pi^{1/2}/8)(g_H/g)^{1/2} \quad (25)$$

to estimate R_H from the measured R_g data for each polymer. It is known that R_{Hl}/R_{gl} is insensitive to the difference in chain statistics (ideal chains vs excluded-volume chains), as is the ratio of the root-mean-square end-to-end distance of a linear polymer to its R_g.[25] Therefore, it is expected that the above procedure to estimate R_H from the measured R_g will not introduce a significant error.

Parts a and b of Figure 6 compare the calibration curves by R_g and R_H, respectively. Different symbols denote different chain architectures. Apparently, the universality is better in the calibration by R_H. In fact, it is comparable to the calibration by the hydrodynamic volume which is shown in ref 5. The universality in the SEC calibration curve by R_H is not surprising, since R_H is close to the cubic root of the hydrodynamic volume per molecule, as stated in section 2.

It will be interesting to examine the calibration by R_H using the values obtained in dynamic light scattering measurements. It will be also interesting to look at the calibration for random copolymers and block copolymers in a solvent good to all constituents. We note that, compared with R_g, measurement of R_H is less susceptible to variations of refractive index contrast with the solvent for different components of the copolymer.

We can regard the universal calibration as a method to estimate R_H for each fraction in an SEC chromatogram. Together with the estimates of R_g and M to be obtained in inline light scattering measurements, we can have g and g_H for each fraction. The two sets of information will allow us to find the architecture of the polymer, since g and g_H can be calculated easily, unlike the ratio for the intrinsic viscosity.

6. Conclusions

Expressions for the partition coefficient of an asymmetric star polymer, a symmetric two-bridge-point polymer, and a comb polymer with a pore of slit geometry were obtained in the form suitable for numerical computation. The partition coefficients calculated for these branching architectures were plotted as a function of the ratio of the chain dimension to the slit width. When the hydrodynamic radius was used for the chain dimension rather than the radius of gyration, these plots nearly overlapped. The result indicates that the hydrodynamic radius is superior to the radius of gyration as a measure of the chain dimension in the partitioning with pore.

It is known that the conformation of a rigid-chain polymer approaches that of a linear flexible chain as its contour length increases. It will be interesting to find how the contour length affects the deviation from the universal calibration curve.

Appendix A. R_H of an Asymmetric Star Polymer

For the architecture shown in Figure 1a, the total number of bonds is $N = \sum_{i=1}^{a} N_i$ ($N_i \gg 1$). The formula given by eq 2 is divided into two parts:

$$N^2 R_H^{-1} = \sum_{i=1}^{a} N_i^2 \langle |\mathbf{r}_m - \mathbf{r}_n|^{-1} \rangle_{m,n\in N_i} + \sum_{i\neq j}^{a} N_i N_j \langle |\mathbf{r}_m - \mathbf{r}_n|^{-1} \rangle_{m\in N_i, n\in N_j} \quad (A1)$$

where the first part is for a pair of beads on the same arm and the second part is for the beads on different arms. First calculating $\langle |\mathbf{r}_m - \mathbf{r}_n|^{-1} \rangle$ for given m and n and then averaging it with respect to m and n that are independently and uniformly distributed over [0, N_i], we obtain[12]

$$\langle |\mathbf{r}_m - \mathbf{r}_n|^{-1} \rangle_{m,n\in N_i} = \left(\frac{6}{\pi}\right)^{1/2} \frac{8}{3} N_i^{-1/2} \quad (A2)$$

A similar calculation gives

$$\langle |\mathbf{r}_m - \mathbf{r}_n|^{-1} \rangle_{m\in N_i, n\in N_j} = \left(\frac{6}{\pi}\right)^{1/2} \frac{4}{3N_i N_j} [(N_i + N_j)^{3/2} - N_j^{3/2} - N_i^{3/2}] \quad (A3)$$

From eqs A1 to A3, we have

$$R_H^{-1} = \left(\frac{6}{\pi}\right)^{1/2} \frac{8}{3N^2} \{\sum_{i>j} (N_i + N_j)^{3/2} - (a-2)\sum_i N_i^{3/2}\} \quad (A4)$$

For a linear polymer chain with N beads[12]

$$R_{Hl}^{-1} = \left(\frac{6}{\pi}\right)^{1/2} \frac{8}{3} N^{-1/2} \quad (A5)$$

From eqs A4 and A5, the g parameter for R_H is obtained as

$$g_{H,star}^{1/2} = \frac{N^{3/2}}{\sum_{i>j}(N_i + N_j)^{3/2} - (a-2)\sum_i N_i^{3/2}} \quad \text{(A6)}$$

For a symmetric star, eq A6 reduces to $g_{H,star}^{1/2} = a/[(2^{1/2} - 1)(2^{1/2} + a)]$.[12]

Appendix B. R_H of a Symmetric Two-Branch-Point Polymer

For the architecture shown in Figure 1b, possibilities of allocating beads m and n to compute R_H according to eq 2 are classified into the following five cases: (A) two beads are on the same arm; (B) two beads are on different arms of the same branch point; (C) two beads are on arms of different branch points; (D) two beads are on the bridge; and (E) one bead is on the bridge, and the other bead on one of the arms. Counting the numbers of the possibilities, we rewrite eq 2 to

$$R_H^{-1} = \frac{2ar^2}{(1+2ar)^2}\langle|\mathbf{r}_m - \mathbf{r}_n|^{-1}\rangle_A + \frac{2a(a-1)r^2}{(1+2ar)^2}\langle|\mathbf{r}_m - \mathbf{r}_n|^{-1}\rangle_B + \frac{2a^2r^2}{(1+2ar)^2}\langle|\mathbf{r}_m - \mathbf{r}_n|^{-1}\rangle_C + \frac{1}{(1+2ar)^2}\langle|\mathbf{r}_m - \mathbf{r}_n|^{-1}\rangle_D + \frac{4ar}{(1+2ar)^2}\langle|\mathbf{r}_m - \mathbf{r}_n|^{-1}\rangle_E \quad \text{(B1)}$$

where $r = N_1/N_b$ and $\langle\ldots\rangle_\alpha$ denotes the statistical average for case α (α = A, B, C, D, E).

Equations A2 and A3 can be easily adapted for cases A and B. The other three averages are

$$\langle|\mathbf{r}_m - \mathbf{r}_n|^{-1}\rangle_C = \left(\frac{6}{\pi}\right)^{1/2}\frac{4}{3}N_1^{-1/2}r^{-3/2}[(1+2r)^{3/2} - 2(1+r)^{3/2} + 1] \quad \text{(B2)}$$

$$\langle|\mathbf{r}_m - \mathbf{r}_n|^{-1}\rangle_D = \left(\frac{6}{\pi}\right)^{1/2}\frac{8}{3}N_1^{-1/2}r^{1/2} \quad \text{(B3)}$$

$$\langle|\mathbf{r}_m - \mathbf{r}_n|^{-1}\rangle_E = \left(\frac{6}{\pi}\right)^{1/2}\frac{4}{3}N_1^{-1/2}r^{-1/2}[(1+r)^{3/2} - r^{3/2} - 1] \quad \text{(B4)}$$

Therefore, the g parameter for R_H is

$$g_{H,2br}^{1/2} = \frac{(1+2ar)^{3/2}}{2a(a-1)[(2^{1/2}-1)r^{3/2} - (1+r)^{3/2}] + (1+2r)^{3/2}a^2 + (a-1)^2} \quad \text{(B5)}$$

Appendix C. R_H of a Comb Polymer

For the architecture shown in Figure 1c, possibilities of allocating beads m and n to compute R_H according to eq 2 are classified into the following four cases: (A) two beads are on the same arm; (B) two beads are on different arms; (C) two beads are on the backbone; and (D) one bead is on one of the arms, and the other bead on the backbone. Counting the numbers of the possibilities, we rewrite eq 2 as

$$R_H^{-1} = \frac{r^2}{(ar+a+1)^2}a\langle|\mathbf{r}_m - \mathbf{r}_n|^{-1}\rangle_A + \frac{a(a-1)r^2}{(ar+a+1)^2}\langle|\mathbf{r}_m - \mathbf{r}_n|^{-1}\rangle_B + \frac{(a+1)^2}{(ar+a+1)^2}\langle|\mathbf{r}_m - \mathbf{r}_n|^{-1}\rangle_C + \frac{2a(a+1)r}{(ar+a+1)^2}\langle|\mathbf{r}_m - \mathbf{r}_n|^{-1}\rangle_D \quad \text{(C1)}$$

where $r = N_1/N_b$. Equation A2 can be easily adapted for case A. The other averages are

$$\langle|\mathbf{r}_m - \mathbf{r}_n|^{-1}\rangle_B = \left(\frac{6}{\pi}\right)^{1/2}\frac{8}{3a(a-1)}r^{-3/2}N_1^{-1/2}f(r;a) \quad \text{(C2)}$$

$$\langle|\mathbf{r}_m - \mathbf{r}_n|^{-1}\rangle_C = \left(\frac{6}{\pi}\right)^{1/2}\frac{8}{3}(a+1)^{-1/2}r^{1/2}N_1^{-1/2} \quad \text{(C3)}$$

$$\langle|\mathbf{r}_m - \mathbf{r}_n|^{-1}\rangle_D = \left(\frac{6}{\pi}\right)^{1/2}\frac{8}{3a(a+1)}r^{-1/2}N_1^{-1/2}h(r;a) \quad \text{(C4)}$$

where

$$f(r;a) = \sum_{i=1}^{a-1}(a-i)[(2r+i)^{3/2} - 2(r+i)^{3/2} + i^{3/2}] \quad \text{(C5)}$$

$$h(r;a) = \sum_{i=1}^{a}[(r+i)^{3/2} - r^{3/2} - i^{3/2}] \quad \text{(C6)}$$

Therefore, the g parameter for R_H is

$$g_{H,comb}^{1/2} = \frac{(ar+a+1)^{3/2}}{ar^{3/2} + (a+1)^{3/2} + f(r;a) + 2h(r;a)} \quad \text{(C7)}$$

When $r = 1$, eq C7 is identical to the result obtained by Kurata and Fukatsu.[18]

Appendix D. Calculation of $I_{k_1\cdots k_a}$

It can be shown for an odd a that

$$u_{k_1}u_{k_2}\cdots u_{k_a} = \frac{1}{2(2d)^{(a-1)/2}}\sum_{s_1=\pm1}\sum_{s_2=\pm1}\cdots\sum_{s_a=\pm1}(-1)^{(s_1+s_2+\cdots+s_a-1)/2}u_{s_1k_1+s_2k_2+\cdots+s_ak_a} \quad \text{(D1)}$$

where the sign s_i is either 1 or -1. Therefore

$$I_{k_1k_2\cdots k_a} = \frac{1}{\pi}\sum_{s_1=\pm1}\sum_{s_2=\pm1}\cdots\sum_{s_a=\pm1}\frac{(-1)^{(s_1+s_2+\cdots+s_a-1)/2}}{s_1k_1 + s_2k_2 + \ldots + s_ak_a} \quad \text{(D2)}$$

For an even a

$$u_{k_1}\cdots u_{k_a} = \frac{1}{2(2d)^{(a-1)/2}}\sum_{s_1=\pm1}\sum_{s_2=\pm1}\cdots\sum_{s_a=\pm1}(-1)^{(s_1+s_2+\cdots+s_a)/2}v_{s_1k_1 + s_2k_2 + \ldots + s_ak_a} \quad \text{(D3)}$$

where

$$v_k(x) = (2/d)^{1/2}\cos(k\pi x/d) \quad (k = 0, 1, 2, \ldots) \quad \text{(D4)}$$

Therefore

$$I_{k_1 k_2 \cdots k_a} = \frac{1}{2} \sum_{s_1=\pm 1} \sum_{s_2=\pm 1} \cdots \sum_{s_a=\pm 1} (-1)^{(s_1+s_2+\cdots+s_a)/2} \delta_{s_1 k_1 + s_2 k_2 + \cdots + s_a k_a, 0} \quad \text{(D5)}$$

where δ is Kronecker's delta.

References and Notes

(1) Wu, C.-S., Ed.; *Handbook for Size Exclusion Chromatography and Related Techniques*, 2nd ed.; Marcel Dekker: New York, 2004.
(2) Grubisic, Z.; Rempp, P.; Benoit, H. *J. Polym. Sci., Polym. Lett. Ed.* **1967**, *5*, 753.
(3) Malawer, E. G.; Senak, L. In *Handbook for Size Exclusion Chromatography and Related Techniques*, 2nd ed.; Wu, C.-S., Ed.; Marcel Dekker: New York, 2004; Chapter 1, p 1.
(4) Jackson, C.; Barth, H. G. In *Handbook for Size Exclusion Chromatography and Related Techniques*, 2nd ed.; Wu, C.-S., Ed.; Marcel Dekker: New York, 2004; Chapter 4, p 99.
(5) Sun, T.; Chance, R. R.; Graessley, W. W.; Lohse, D. J. *Macromolecules* **2004**, *37*, 4304.
(6) Casassa, E. F. *J. Polym. Sci., Polym. Lett. Ed.* **1967**, *5*, 773.
(7) Casassa, E. F.; Tagami, Y. *Macromolecules* **1969**, *2*, 14.
(8) Zimm, B. H. *J. Chem. Phys.* **1956**, *24*, 269.
(9) Zimm, B. H.; Kilb, R. W. *J. Polym. Sci.* **1959**, *37*, 19.
(10) Radke, W. *Macromol. Theory Simul.* **2001**, *10*, 668.
(11) Radke, W. *J. Chromatogr. A* **2004**, *1028*, 211.
(12) Teraoka, I. *Polymer Solutions: An Introduction to Physical Properties*; John Wiley & Sons: New York, 2002.
(13) Kirkwood, J. G. *J. Polym. Sci.* **1954**, *12*, 1.
(14) van Vliet, J. H.; Luyten, M. C.; ten Brinke, G. *Macromolecules* **1992**, *25*, 3802.
(15) Cifra, P.; Bleha, T. *Macromol. Theory Simul.* **1999**, *8*, 603.
(16) Giddings, J. C.; Kucera, E.; Russell, C. P.; Myers, M. N. *J. Phys. Chem.* **1968**, *72*, 4397.
(17) Teraoka, I. *Prog. Polym. Sci.* **1996**, *21*, 89.
(18) Kurata, M.; Fukatsu, M. *J. Chem. Phys.* **1964**, *41*, 2934.
(19) Graessley, W. W. *Polymeric Liquids and Networks: Structure and Properties*; Taylor & Francis: New York, 2004.
(20) Zimm, B. H.; Stockmayer, W. H. *J. Chem. Phys.* **1949**, *17*, 1301.
(21) Berry, G. C. *J. Polym. Sci., Part A-2* **1968**, *6*, 1551.
(22) Cifra, P.; Teraoka, I. *Polymer* **2002**, *43*, 2409.
(23) Teraoka, I.; Wang, Y. *J. Chem. Phys.* **2001**, *115*, 1105.
(24) Casassa, E. F. *Macromolecules* **1976**, *9*, 182.
(25) des Cloizeaux, J.; Jannik, G. *Polymers in Solution: Their Modeling and Structure;* Clarendon: Oxford, 1990.

MA0494939